

## Reflection functions of pipes

T. Trommer<sup>1,2</sup>, H.J. Ausserlechner<sup>1,2</sup>, J. Angster<sup>2,1</sup>, A. Miklós<sup>3</sup>

<sup>1</sup> Universität Stuttgart, Lehrstuhl für Bauphysik, D-70569 Stuttgart

<sup>2</sup> Fraunhofer-Inst. Bauphysik, Nobelstraße 12, D-70569 Stuttgart, Email: Trommer@ibp.fraunhofer.de

<sup>3</sup> Steinbeis Transferzentrum Angewandte Akustik, D-70499 Stuttgart, Email: stz746@stw.de

### Introduction

The sound an organ pipe radiates is predominantly influenced by the resonator. In it sound waves travel back and forth between the lower end (consisting of upper lip, pipe mouth, languid) and the upper end being partially reflected as well as radiated from each of these ends. These reflections and herewith directly the pipe sound is dependent on different properties of which mainly contributing factors are the geometry of the resonator in size and shape (cylindrical, conical, diameter, length) as well as the attributes of the ends (open, closed, tuning geometries, mouth size, etc.).

The first sound signal excites the stationary air column defined by the resonator. The reflected part of the sound signal from the upper end after being reflected from the lower end superimposes with the periodic sound emitted continuously by the sound source. In optimum this retroactivity leads to a steady state of the resonant circuit of which the open ends radiate the corresponding organ pipe sound.

In order to model the resonant part of a pipe the reflection functions of both ends in dependency of the geometries are needed. These will be gathered by an especially developed method by means of time domain measurements on pipes with corresponding dimensions to in-situ employed organ pipes.

### Pulse reflectometry on 4ft. organ pipes

Previous publications used pulse reflectometry not only to analyze tubes and series of tubes [1], but also to characterize whole instruments (see [2], [3] and [4]) or human airways (see [5] and [6]). The setups and applications all have in common a source tube of a couple meters in length (up to 25m) and a diameter smaller than 15mm. These dimensions however do not correspond at all with any dimensioning of organ pipes. A standard 4ft. pipe roughly has following sizes: length of 130cm, diameter of 92.5mm. In an organ pipe therefore the first transversal modes will be excited at corresponding lower frequencies. Furthermore an organ pipe does not have a simple input to the resonant chamber, as for example other musical instruments or respectively an output as the human airway does. Therefore a simple, fixed source tube set-up as mentioned in the references could not be applied. Fortunately the acoustic relevant - sound modifying - parts of an organ pipe resonator are concentrated at the upper end and at the mouth of the organ pipe respectively. For that reason solely these areas need to be analyzed with the pulse reflectometry method. This will be done in two separate measurements allowing the instrument to be its own, however much shorter, source tube leading to a completely new measurement technique. From the languid

detached resonators are employed, which in combination with a pipe-foot model resembles a complete organ pipe. In order to separate incoming and reflected pulses a short pulse length with no ringing of the source was essential. The former however is, in conjunction with the demand for a high bandwidth a tradeoff in regard to the excited transversal modes.

### Measurement setup

The source (S) is an Etymotic ER 3A speaker driven with a 2kHz Haversine 5Vpp single burst at a repetition rate of 50ms. The pulse rate is as high as possible, in favor of the speed of the measurement, however as low as necessary so that the reverberation of the last pulse does not interfere with the measurement of the next pulse. The source is mounted opposite the end of interest and held in place at the center of the tube by damping material (D). Between the source and the microphone (M) additional damping (D) has been placed to reduce the amplitudes of transversal modes. A schematic of the setup is given in Figure 1. The microphone (Sennheiser KE 4-221-2) is placed at half length of the tube in order to maximize the separation in the time domain of the incoming pulses from reflected pulses as well as the first reflection from the end of interest from possible further reflections coming from the source end. The signals are amplified using a PA-LAB-2MC microphone amplifier and digitalized at 50 kHz using a LeCroy Waverunner 64Xi averaging over 1000 pulses for one measurement. Further treatment of the measurements was done mathematically.

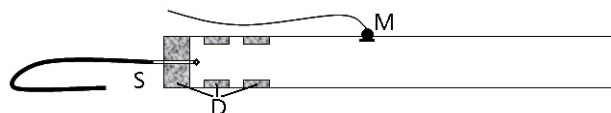


Figure 1: Setup of a tube for impulse measurements (S: source, D: damping element, M: microphone)

### Mathematical treatment

In the time domain the reflected wave  $a(t)$  can be described as a convolution of the incoming wave  $i(t)$  with the reflection function  $r(t)$  corresponding to the reflecting area. However, calculating the time domain deconvolution to measured signals directly is not easy [7]. Therefore here an approach using the frequency domain is applied. Equation (1) describes this basic connection for the time domain and its transformation into the frequency domain.

$$i(t) * r(t) = a(t) \Leftrightarrow I(f) \cdot R(f) = A(f) \quad (1)$$

Solving this equation for the reflection factor in the frequency domain  $R(f)$  and then calculating the inverse Fourier transform of this simply gives the reflection factor in the time domain. However, here as well, the simplicity of the

theory finds some boundaries. The amplitudes of the small noise floor at frequencies not excited by the pulses can become very large when dividing and therefore lead to significant errors when  $R(f)$  is calculated. In order to minimize the arising errors following possibility has turned out to be useful [8]:

The addition of a constraining factor  $q$  to the denominator to prevent division by zero. (Eq. (2))

$$R(f) = \frac{A(f)I^*(f)}{I(f)I^*(f) + q} \quad (2)$$

$I^*(f)$  denotes the complex conjugate of  $I(f)$ . In case the bandwidth of the input pulse is equal to, or greater than the Nyquist frequency of the sampling frequency the constraining factor  $q$  can be set to zero because the pulse will contain sufficient energy at all measured frequencies. A plot of  $I(f)$  is given in Figure 2.

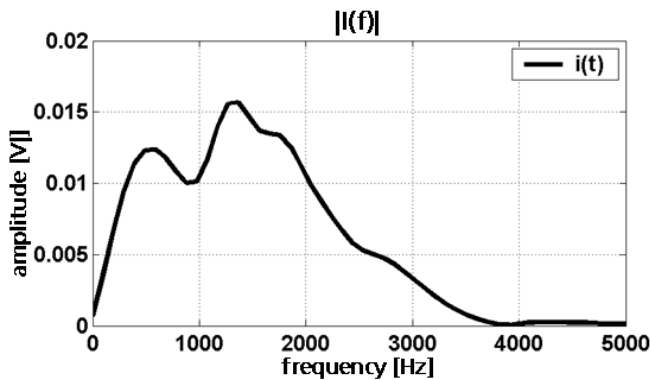


Figure 2: Spectra of the incoming pulse

### Measurements

The measurements were all carried out in the anechoic room of the Fraunhofer Institut Bauphysik, Stuttgart. In this paper two measurement rows on an organ pipe with a diameter of 83mm and a length of approximately 120cm will be presented. In measurement row A the end of interest of the resonator was stepwise closed off with a sheet of metal, see Figure 3. In measurement row B, as depicted in Figure 10, a closed end of a pipe was stepwise cut open at the side of the pipe herewith resembling the cut up and languid of an organ pipe. For each row of measurements it was important that the source, the damping around the source and microphone were placed inside the pipe and not changed for the duration of the measurements. The relative short tube length of the resonator results that a clear time wise separation of input and reflected pulse is not possible an a calibration measurement is needed. For this the incoming pulse is measured once using an extension tube, herewith separating the pulse from the first reflections. During further measurements the input pulse is always crosschecked with this measurement in order to certify the unvaried manner of the excitation and the microphone position. From the measurements with the reflection pulse the calibration measurement with the incoming wave is subtracted in order to remove any superimposed movements of the not yet decayed input pulse. From both measurements the time

period of the pulses are extracted with the main pulse in the middle of the considered period, which in our case smaller than 8ms because it is limited by further reflections. The evaluation of the averaged input pulse is the same as for the averaged reflected pulses. In order to be self windowing signals for the fast-Fourier transform (fft) both are multiplied with a Hanning window the size of the data before a 1024 point fft is calculated. The treatment of the data of the frequency domain according to equation (2) and the calculation of the inverse fast-Fourier transform (ifft) gives the reflection function in the time domain  $r(t)$ . Generally the result is of complex nature, however in these cases the imaginary parts are neglectably small in comparison to the real parts (by a factor of  $10^{16}$ ) and will be omitted.

### Measurement row A

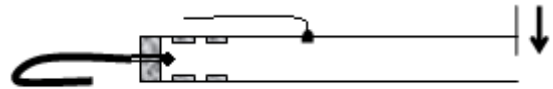


Figure 3: Setup for measurement row A

In this measurement the open end of the pipe was closed off in step sizes of 5mm with a rigid even metal plate. The sides of the plate connected to the pipe were sealed with gum. Already with this rather simple measurement in the time domain, comparing Figure 4 and Figure 5, certain properties concerning reflections are clearly visible. For a reflection on a closed end  $a(t)$  is very similar to  $i(t)$ . Roughly one can say that the  $R(f) \approx 1$  independent of the frequency. For a reflection on an open end this conclusion can not be so easily made.  $a(t)$  in comparison with  $i(t)$  is present with a roughly  $180^\circ$  phase shift and clearly decreased amplitudes. Latter can be explained with the radiation of energy from the open end of the pipe. All in all leading to following assumption for the open end  $0 > R(f) > -1$ .

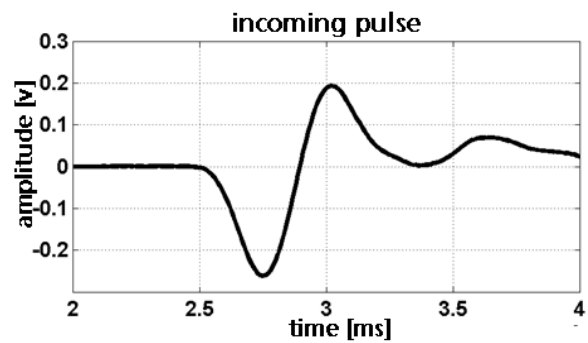


Figure 4: Incoming pulse of measurement row A

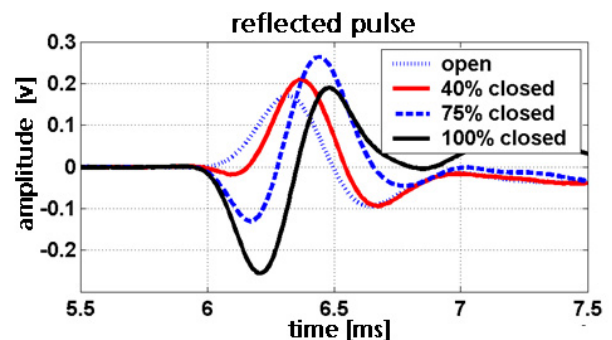


Figure 5: Reflected pulses of measurement row A

When examining  $a(t)$  for different openings a steady transition from open to closed can be clearly seen. Independent of the actual properties of the opening at the end of the pipe  $a(t)$  can be expressed as a linear addition of reflections from an open respectively a closed end with corresponding amplitude adjustments.

The calculated complex reflection function  $R(f)$  can also be interpreted as the complex input impedance of the upper end of the pipe. In this form as depicted in Figure 6 and Figure 7 the steady transition of the results between the open and closed reflection can be seen. The above mentioned  $R(f) \approx 1$  for reflection of a closed end is confirmed and the assumption for the reflection of the open end holds true for frequencies lower than 2.2kHz.

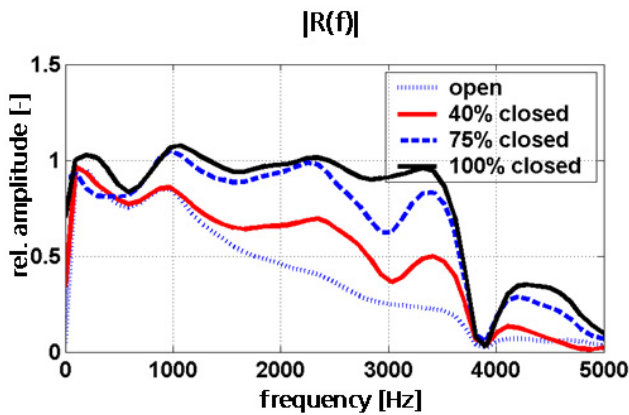


Figure 6: Absolute of the complex reflection function of measurement row A

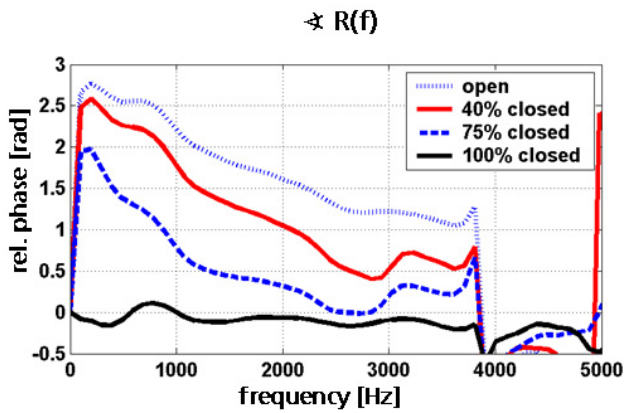


Figure 7: Angle of the complex reflection function of measurement row A

Finally the reflection function in the time domain  $r(t)$  is calculated. This leads to the curves plotted in Figure 8.

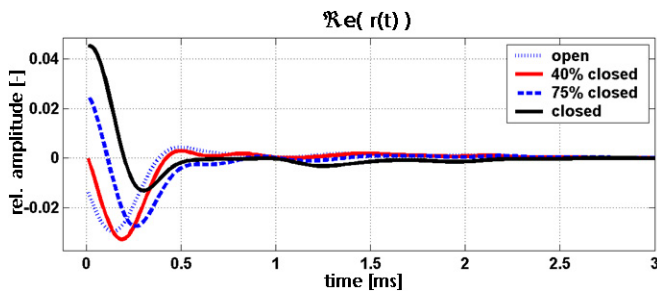


Figure 8: Reflection function of measurement A in the time domain

The main information on the reflection are given in the first millisecond of  $r(t)$ . Reflections off a closed end are convolved with a signal of positive decaying amplitude right at the beginning. Reflections off an open pipe end are convolved with a signal of negative amplitude which increases absolutely at first before decreasing. This time delay at the open end may explain geometrically the effect of the end-corrections of open pipes. As with all previous curves the steady tendency of the curves with varying termination of the pipe can be seen here as well. In order to give a better overview and a better comparison to measurement B, all results of  $r(t)$  (with  $q=0.0001$ ) have been plotted in Figure 9.

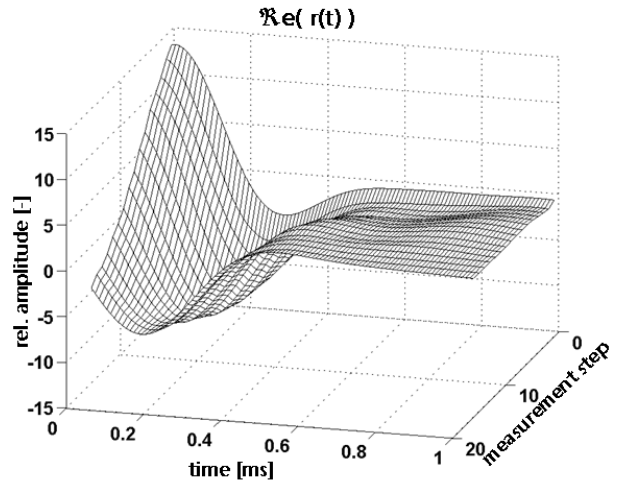


Figure 9: Complete results for the reflection function in the time domain of measurement A

### Measurement row B

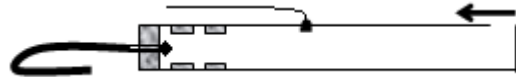
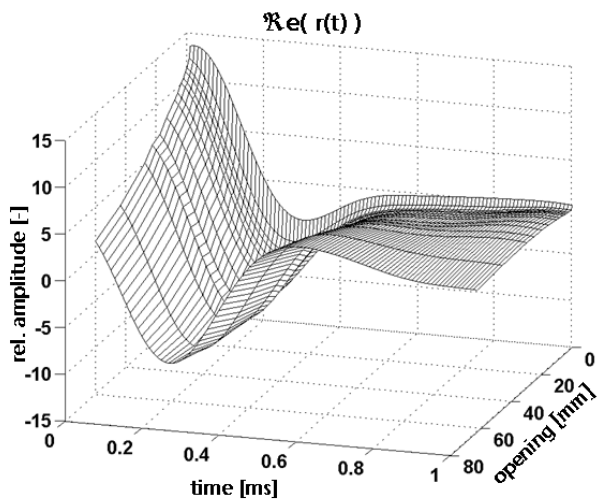


Figure 10: Setup for measurement row B

For this measurement row after the measurement with the extension pipe, the upper end of the pipe was soldered closed. Cut ups with increasing height were cut into the side of the pipe. The width of the cut up was chosen to be approximately one fourth, the main cut up height of interest as one sixteenth of the circumference of the pipe in order to resemble dimensioning of organ pipes. The first cut ups were chosen to be of smaller incremental size as the cut ups past the height of interest. The results of the reflection function in the time domain (with  $q=0.0001$ ) are shown in Figure 11. At first glance the results seem similar an steady transitions from a cut up of 0mm to 60mm can be clearly seen. In the setup of measurement row B the end of interest is always present with an area of closed reflection (perpendicular to the movement of the travelling pulse) and the area of open reflection (parallel to the movement travelling pulse) is located closer to the source for higher cut ups. Therefore with superposition of hard and open reflections in order to calculate intermediate reflections the time difference between the areas of hard respectively open reflections needs to be accounted for. The dominant closed reflection leads to the fact that the reflection function in the time domain

always starts off with positive, decreasing amplitude. The absolute maximum amplitude however varies depending on the size of the cut up and with a cutup of 60mm it is clearly negative with a time delay as previously discussed in measurement row A.



**Figure 11:** Complete results for the reflection function in the time domain of measurement row B

## Conclusion

A method for evaluating the reflection functions in the time domain by means of measurements on pipe dimensions of 4ft. organ pipes has been developed and successfully been carried out. Both parts of a pipe which play a major role on the sound modification, the upper and the mouth of the pipe respectively, can be measured using time domain impulse reflectometry.

Basic principles concerning reflections could be validated with this procedure. The prospect of linking the reflection function, the input impedance, the radiation of pipes and for example the end correction of pipes with each other showed by means of this one measurement gives an outline of the far reaching possibilities this simple approach has.

As a next step the effect of the diameter of the pipes as well as the damping will be measured and all of the results will be formulated mathematically in order to give a simpler description of the revealed physical properties of the reflection from an arbitrarily ending pipe.

## References

- [1] J. D. Polack, X. Meynial, J. Kergomard, C. Cosnard, M. Bruneau: Reflection function of a plane sound wave in a cylindrical tube. *Revue Phys. Appl.* **22** (1987), 331-337
- [2] D. H. Keefe: Wind-instrument reflection function measurements in the time domain. *JASA* **99** (1996), 2370-2381
- [3] A. P. Watson, J. M. Bowsher: Impulse Measurements on Brass Musical Instruments. *ACUSTICA* **66** (1988), 170-174
- [4] D. B. Sharp: Acoustic pulse reflectometry for the measurement of musical wind instruments. PhD University of Edinburgh (1996)
- [5] I. Marshall, M. Rogers, G. Drummond: Acoustic reflectometry for airway measurement. Principles, limitations and previous work. *Clin. Phys. Physiol. Meas.* **Vol.12, No.2** (1991), 131-141
- [6] Man Mohan Sondhi, J. R. Resnick.: The inverse problem for the vocal tract: Numerical methods, acoustical experiments, and speech synthesis. *JASA* **73** (1983), 985-1002
- [7] J. Agulló, S. Cardona, D. H. Keefe.: Time-domain deconvolution to measure reflection functions for discontinuities in waveguides. *JASA* **97** (1995), 1950-1957
- [8] D. B. Sharp; D. M. Campbell: Leak detection in pipes using acoustic pulse reflectometry. *ACUSTICA* **83** (1997), 560-566

## Acknowledgement

This research is supported by the Deutsche Forschungsgemeinschaft (DFG) with the project "Development of a physical model for computer simulated production of the sound of a labial organ pipe" (Sb SE 1561/1-1).